Numerical simulations of coupling effects in FGM plates by meshfree methods

***V. Sladek[1], L. Sator[1], M. Repka[1], J. Sladek[1]**

[1]Institute of Construction and Architecture, Slovak Academy of Sciences, Bratislava, Slovakia

* Corresponding and Presenting author: vladimir.sladek@savba.sk

Abstract

The paper deals with derivation of 2D formulation as well as numerical implementation and study of coupling effects in elastic functionally graded material (FGM) plates within the theory of stationary thermo-elasticity. Unified formulation is developed with involving the assumptions used in the classical Kirchhoff-Love theory for bending of thin elastic plates as well as the assumptions used in the shear deformation plate theory of the 1st and 3rd order. The governing equations and the boundary conditions for deformations are derived from the variational principle, while the formulation for thermal problem is derived by averaging the 3D heat conduction formulation with respect to the transversal direction. The strong formulation and meshless approximation are developed for the derived formulation. The coupling effects are studied by numerical simulations in FGM plates with possible variable thickness and subject to three kinds of stationary loading: (i) uniform transversal loading; (ii) simple tension in plane of the plate; (iii) prescribed different temperatures on the bottom and top surfaces of the plate.

Keywords: **Stationary thermo-elasticity, continuous inhomogeneity, plate bending, 2D formulation, coupling effects, numerical study**

Introduction

Plate structures are attracting attention of engineers, designer and researchers for a long time because of their superior properties and new features appearing with development of new materials. Due to the small aspect ratio of thickness to in-plane dimensions, in the plate theories the 3D formulation of elasticity problem is assumed in semi-integral form with integration across the plate thickness, and resulting into simplified 2D problems. In stationary thermo-elasticity [1], the temperature field is independent of elastic fields, though it is not valid in reverse. Thus, the thermal problem can be solved separately in advance and one can utilize the obtained temperature field in evaluation of the semi-integral fields occurring in the governing equations for bending problem. For this purpose, it is necessary to replace the Hooke law by the Duhamel-Neumann constitutive law known from the theory of thermo-elasticity [1]. In general, however, we don't know the temperature field in terms of integrable functions and the 2D formulation for bending of plates with including thermal effects cannot be derived in closed form. Therefore the development of 2D formulation for thermal problems in plates is desired.
Functional gradation of material coefficients and/or variable thickness of the plate represent another reason why the correct formulation for plate problems must be derived for FGM plates by performing the integration with respect to the transversal coordinate in the variational formulation of the original 3D thermo-elasticity problem. The FGM composites [11-15] have significant utilization in design of structural elements not only because of superior properties of micro-constituents but also for elimination of interface discontinuities occurring in laminated composite structures [16]. The most frequently used modeling of functional variation of material coefficients is the rule of mixture where the material coefficients of multiphase

materials are related directly to the volume fractions and individual coefficients of the constituents. Besides several rather simple models for spatial gradation of volume fractions by analytical functions, there have been developed also more sophisticated models (see e.g. [17-19]) for spatial distribution of volume fractions with including some microstructural aspects of constituents of micro/nano-composites. In this paper, we confine to simple power-law gradations of material coefficients in two-constituent composites, in order to demonstrate some new coupling effects due to gradation of material coefficients and/or plate thickness.

In the most simplified theory, the Kirchhoff-Love theory (KLT), the shear deformations are omitted. There have been developed also generalized shear deformation theories including the 1st order shear deformation theory (FSDPT) [16, 20] and higher order shear deformation theories (HSDPT) [16, 20-23], which account for transverse shear strains and stresses in contrast to the KLT. In this paper, starting from the principle of virtual work and assuming the power-law gradation in the transversal direction, the dependence of all elasticity fields on the transversal coordinate is known a priori and the integrations along the direction of gradation can be accomplished analytically in closed form. Thus, the original 3D problems is converted to 2D problem with correctly derived governing equations and boundary conditions. In stationary thermoelasticity, the temperature field is not influenced by the elasticity fields and the thermal problem can be solved separately. In order to get the 2D formulation also for thermal problem in plates, we consider the power series expansion of the temperature field with respect the transversal coordinate up to the 2nd power, which is physically meaningful as long as the plate thickness is significantly smaller than its characteristic length in the mid-plane of the plate. Having known the dependence of thermal fields on the transversal coordinate, we can consider the 3D heat conduction equation in the averaged sense. This 2D governing equation together with the boundary conditions on the bottom and top surfaces of the plate play the role of governing equations for primary thermal fields. The complete 2D formulation for plate bending in stationary thermo-elasticity is discretized by using the meshless Moving Least Square approximation (MLS) [5-8] for spatial variations of all 2D field variables. Since the governing equations are represented by the partial differential equations (PDE) with variable coefficients and the accuracy of approximation of derivatives is decreasing with increasing their order, we decomposed the original PDE of the 4th order into the system of PDE with 2nd order derivatives by introducing new field variables, in order to eliminate high order derivatives. To facilitate the numerical solution as much as possible for the considered system of the PDE with variable coefficient, we propose to use strong formulation, which is free of any integrations and reduces the amount of evaluations of shape functions, since the evaluations are localized to nodal points. The numerical simulations are employed for study of coupling effects in FGM plates with possible variable thickness and subject to three kinds of stationary loading: (i) uniform transversal loading; (ii) simple tension in plane of the plate; (iii) prescribed different temperatures on the bottom and top surfaces of the plate.

2D formulation of bending problems for FGM plates in stationary thermo-elasticity

It is well known that in stationary thermo-elasticity [1], the temperature field is not affected by mechanical fields, while in linear theory the thermal strains are proportional to the deviation of temperature from its value at the reference state $e_{kl}^{\theta}(\mathbf{x},z)=\alpha\left(\theta-\theta_0\right)\delta_{kl}$, with α being the linear thermal expansion coefficient. Therefore the thermal problem can be solved separately in advance and subsequently the elasticity problem can be solved with bearing in mind thermal strains known from the solution of thermal problem. Evidently, the thermo-elasticity problem is reduced to a pure elasticity problem, if either the temperature is kept on the reference θ_0 value or $\alpha=0$.

It is well known that the original 3D elasticity problem for plate structures can be reduced to 2D problem because of significantly smaller thickness than the other in-plane length dimensions. According to assumptions adopted for deformation of plates, several theories have been developed for bending of elastic plates. Among the most frequently applied theories to bending of elastic plates, one can name the Kirchhoff-Love theory for bending of thin elastic plates (KLT), and the shear deformation theories of the 1st and 3rd order (FSDPT, TSDPT). Recall that a unified formulation can be developed for bending of elastic plates with possibility to switch between three above mentioned theories by selecting proper values for two key factors [2],[3]. Without going into details, we outline the derivation of the unified formulation for bending of FGM plates within stationary thermo-elasticity. The three components of displacements $v_i(\mathbf{x},x_3)$ can be expressed in terms of the in-plane displacements $u_\alpha(\mathbf{x})$, transversal displacements (deflections) $w(\mathbf{x})$ and rotations of the normal to the mid-surface $\varphi_\alpha(\mathbf{x})$ as

$$v_i(\mathbf{x},x_3,t) = \delta_{i\alpha}\left\{u_\alpha(\mathbf{x},t) + \left[c_1\phi(x_3) - x_3\right]w_{,\alpha}(\mathbf{x},t) + c_1\phi(x_3)\varphi_\alpha(\mathbf{x},t)\right\} + \delta_{i3}w(\mathbf{x},t) \tag{1}$$

where $\phi(x_3) := x_3 - c_2\psi(x_3)$, $\psi(x_3) := \frac{4}{3}\left(\frac{x_3}{h}\right)^2 x_3$, $x_3 \in [-h/2,\ h/2]$, $\mathbf{x} \in \Omega$

$$c_1 = \begin{cases} 0, & \text{KLT} \\ 1, & \text{SDPT} \end{cases}, \qquad c_2 = \begin{cases} 0, & \text{FSDPT, KLT} \\ 1, & \text{TSDPT} \end{cases}.$$

The Latin subscripts can take values $\{1,2,3\}$, while the Greek ones $\{1,2\}$. If we denote the characteristic length in the mid-surface Ω as L, the expression (1) is based on the assumption $h/L \ll 1$. Taking into account the thermal strains and the total strains $e_{ij} = \left(v_{i,j} + v_{j,i}\right)/2$ together with Hooke's law, one can write the stress tensor components as

$$\sigma_{\alpha\beta}(\mathbf{x},x_3) = \frac{E}{1-\nu^2}\frac{1-\nu}{H}\left[\tau^{(u)}_{\alpha\beta}(\mathbf{x}) + c_1\phi(x_3)\tau^{(\varphi)}_{\alpha\beta}(\mathbf{x}) + \left(c_1\phi(x_3) - x_3\right)\tau^{(w)}_{\alpha\beta}(\mathbf{x}) - \alpha\tau^{(\theta)}_{\alpha\beta}(\mathbf{x},x_3)\right] \tag{2}$$

$$\sigma_{\alpha 3}(\mathbf{x},x_3) = \frac{E}{1+\nu}\frac{c_1}{2}\phi'(x_3)\left[w_{,\alpha}(\mathbf{x}) + \varphi_\alpha(\mathbf{x})\right]$$

$$\sigma_{33}(\mathbf{x},x_3) = \frac{E\nu}{1-\nu^2}\frac{1-\nu}{H}\left[u_{\gamma,\gamma}(\mathbf{x}) + c_1\phi(x_3)\varphi_{\gamma,\gamma}(\mathbf{x}) + \left(c_1\phi(x_3) - x_3\right)w_{,\gamma\gamma}(\mathbf{x}) - \alpha\frac{1+\nu}{\nu}\left(\theta(\mathbf{x},x_3) - \theta_0\right)\right]$$

where

$$\tau^{(u)}_{\alpha\beta}(\mathbf{x}) := H\left(u_{\alpha,\beta}(\mathbf{x}) + u_{\beta,\alpha}(\mathbf{x})\right)/2 + \nu\delta_{\alpha\beta}u_{\gamma,\gamma}(\mathbf{x}) \tag{3}$$

$$\tau^{(\varphi)}_{\alpha\beta}(\mathbf{x}) := H\left(\varphi_{\alpha,\beta}(\mathbf{x}) + \varphi_{\beta,\alpha}(\mathbf{x})\right)/2 + \nu\delta_{\alpha\beta}\varphi_{\gamma,\gamma}(\mathbf{x})$$

$$\tau^{(w)}_{\alpha\beta}(\mathbf{x}) := Hw_{,\alpha\beta}(\mathbf{x}) + \nu\delta_{\alpha\beta}w_{,\gamma\gamma}(\mathbf{x}), \quad \tau^{(\theta)}_{\alpha\beta}(\mathbf{x},x_3) := (1+\nu)\left(\theta(\mathbf{x},x_3) - \theta_0\right)\delta_{\alpha\beta}$$

are strain contributions corresponding to in-plane displacements, rotations, deflections, and temperature, respectively. Furthermore, E and ν stand for the Young modulus and Poisson ratio, while

$$H = \begin{cases} 1-\nu, & \text{plane stress problems} \\ 1-2\nu, & \text{otherwise} \end{cases}.$$

The Young modulus and linear thermal expansion coefficient are allowed to be continuous functions of position with assuming the power-law gradation in the transversal direction as

$$E(\mathbf{x},x_3) = E_0 E_H(\mathbf{x}) E_V(x_3), \qquad E_V(x_3) = 1 + \zeta\left(\frac{1}{2} \pm \frac{x_3}{h}\right)^p \tag{4}$$

$$\alpha(\mathbf{x},x_3)=\alpha_0\alpha_H(\mathbf{x})\alpha_V(x_3)\,,\qquad \alpha_V(x_3)=1+\xi\left(\frac{1}{2}\pm\frac{x_3}{h}\right)^r,$$

which result from utilization of rule of mixture for two-constituent micro-composite and the power-law gradation of volume fractions in the transversal direction. Moreover, the thickness of the plate is allowed to be variable on the in-plane coordinates, $h(\mathbf{x})$.

Since the dependence of mechanical fields on x_3 is known a priori, the pure elasticity 3D problem can be converted to 2D problem. In order to extend such a possibility to thermo-elastic problems, we should know also the dependence of temperature on the transversal coordinate prior to solving the 3D thermal boundary value problem. In thin structures ($h/L\ll 1$), it is physically reasonable to simulate the distribution of the temperature field by using the power series expansion

$$\theta(\mathbf{x},x_3)\approx\theta_0+\vartheta_0(\mathbf{x})+z\vartheta_1(\mathbf{x})+z^2\vartheta_2(\mathbf{x})\,,\qquad z=\frac{x_3}{h}\in[-0.5,\ 0.5] \tag{5}$$

in which the new fields $\vartheta_s(\mathbf{x})$ for ($s=0,1,2$), are variable in the plate mid-plane. In view of (3) and (5), we obtain

$$\tau_{\alpha\beta}^{(\theta)}(\mathbf{x},x_3)=\sum_{s=0}^{2}z^s\tau_{\alpha\beta}^{(\vartheta_s)}(\mathbf{x})\ ,\qquad \tau_{\alpha\beta}^{(\vartheta_s)}(\mathbf{x}):=(1+\nu)\vartheta_s(\mathbf{x})\delta_{\alpha\beta}\ . \tag{6}$$

Now, the variational formulation of the mechanical part of the original 3D thermoelacticity problem is given by the principle of virtual work

$$\delta U-\delta W_e=0\,,\qquad \delta U=\int_\Omega\left(\int_{-h/2}^{h/2}\sigma_{ij}(\mathbf{x},x_3)\delta e_{ij}(\mathbf{x},x_3)dx_3\right)d\Omega \tag{7}$$

$$\delta W_e=\int_\Omega\bar{t}_3(\mathbf{x})\delta w(\mathbf{x})d\Omega+h(\mathbf{x})\int_{\partial\Omega}\bar{t}_\alpha(\mathbf{x})\delta u_\alpha(\mathbf{x})d\Gamma$$

in which the work of external forces is represented by the transversal loading $\bar{t}_3(\mathbf{x})$ applied on the top/bottom surfaces, and $\bar{t}_\alpha(\mathbf{x})$ are in-plane tractions applied on the lateral surfaces of the plate. The integration with respect to x_3 can be performed analytically and we obtain the 2D formulation given by governing equations at $\mathbf{x}\in\Omega$:

$$T_{\alpha\beta,\beta}(\mathbf{x})=0 \tag{8}$$

$$M_{\alpha\beta,\alpha\beta}^{(w)}(\mathbf{x})+T_{3\beta,\beta}^{(w\varphi)}(\mathbf{x})=-t_3(\mathbf{x})$$

$$M_{\alpha\beta,\beta}^{(\varphi)}(\mathbf{x})-T_{3\alpha}^{(w\varphi)}(\mathbf{x})=0$$

and boundary restrictions (possible boundary conditions) at $\mathbf{x}\in\partial\Omega$:

$$\left[n_\beta(\mathbf{x})T_{\alpha\beta}(\mathbf{x})-h\bar{t}_\alpha(\mathbf{x})\right]\delta u_\alpha(\mathbf{x})=0\ \Rightarrow\ n_\beta(\mathbf{x})T_{\alpha\beta}(\mathbf{x})-h\bar{t}_\alpha(\mathbf{x})=0\ \text{ or }\ u_\alpha(\mathbf{x})=\bar{u}_\alpha(\mathbf{x}) \tag{9a}$$

$$n_\alpha(\mathbf{x})n_\beta(\mathbf{x})M_{\alpha\beta}^{(w)}(\mathbf{x})\delta\left(\frac{\partial w}{\partial\mathbf{n}}(\mathbf{x})\right)=0\ \Rightarrow\ n_\alpha(\mathbf{x})n_\beta(\mathbf{x})M_{\alpha\beta}^{(w)}(\mathbf{x})=0\ \text{ or }\ \frac{\partial w}{\partial\mathbf{n}}(\mathbf{x})=0 \tag{9b}$$

$$n_\beta(\mathbf{x})M_{\alpha\beta}^{(\varphi)}(\mathbf{x})\delta\varphi_\alpha(\mathbf{x})=0\ \Rightarrow\ n_\beta(\mathbf{x})M_{\alpha\beta}^{(\varphi)}(\mathbf{x})=0\ \text{ or }\ \varphi_\alpha(\mathbf{x})=0 \tag{9c}$$

$$V(\mathbf{x})\delta w(\mathbf{x})=0\ \Rightarrow\ V(\mathbf{x})=0\ \text{ or }\ w(\mathbf{x})=0 \tag{9d}$$

where

$$V(\mathbf{x}) := n_\alpha(\mathbf{x})\left(M^{(w)}_{\alpha\beta,\beta}(\mathbf{x}) + T^{(w\varphi)}_{3\alpha}(\mathbf{x})\right) + \frac{\partial}{\partial \mathbf{t}} T^{(w)}(\mathbf{x}) - \sum_c \delta(\mathbf{x}-\mathbf{x}^c)\left[\!\left[T^{(w)}(\mathbf{x}^c)\right]\!\right]$$

is the generalized shear force and the following semi-integral fields have been introduced by the definitions

$$T_{\alpha\beta}(\mathbf{x}) := \int_{-h/2}^{h/2} \sigma_{\alpha\beta}(\mathbf{x}, x_3)dx_3 \ , \tag{10}$$

$$M^{(\varphi)}_{\alpha\beta}(\mathbf{x}) := c_1 \int_{-h/2}^{h/2} \phi(x_3)\sigma_{\alpha\beta}(\mathbf{x}, x_3)dx_3 \ , \qquad M^{(w)}_{\alpha\beta}(\mathbf{x}) := \int_{-h/2}^{h/2} \left(x_3 - c_1\phi(x_3)\right)\sigma_{\alpha\beta}(\mathbf{x}, x_3)dx_3 \ ,$$

$$T^{(w\varphi)}_{3\beta}(\mathbf{x}) := c_1 \int_{-h/2}^{h/2} \left\{\left[(1-c_2)\kappa + c_2\right] - c_2\psi'(x_3)\right\}\sigma_{3\beta}(\mathbf{x}, x_3)dx_3$$

where the shear correction factor κ has been introduced as the Reissner modification of the shear stresses in order to be predicted a correct amount of energy in the case of the FSDPT ($c_1 = 1 \wedge c_2 = 0$). Furthermore, the twisting moment has been introduced as

$$T^{(w)}(\mathbf{x}) := t_\alpha(\mathbf{x}) n_\beta(\mathbf{x}) M^{(w)}_{\alpha\beta}(\mathbf{x}) \tag{11}$$

and the jump at a corner point on the oriented boundary edge is defined as

$$\left[\!\left[A(\mathbf{x}^c)\right]\!\right] := A(\mathbf{x}^c + 0) - A(\mathbf{x}^c - 0) \ .$$

The explicit expressions for semi-integral fields are given in Appendix, since the integrations prescribed in (10) can be performed in closed form. Substituting (A.2) into (8) and (9), one obtains the governing equations and the possible boundary conditions in terms of primary fields and their derivatives.

Up to now, we have supposed that the temperature is known from the solution of stationary thermal problem. Now, we need to derive the governing equations and boundary conditions for particular fields $\vartheta_s(\mathbf{x})$ defined in Eq. (5) with starting from the 3D formulation, where the heat conduction equation is given by the PDE

$$\left(k(\mathbf{x}, x_3)\theta_{,j}(\mathbf{x}, x_3)\right)_{,j} = 0 \tag{12}$$

in which k is the heat conduction coefficient, which is prescribed by continuous functions in FGM. In accordance with above mentioned assumptions, we consider

$$k(\mathbf{x}, x_3) = k_0 k_H(\mathbf{x}) k_V(x_3) \ , \qquad k_V(x_3) = 1 + \omega\left(\frac{1}{2} \pm \frac{x_3}{h}\right)^s \ . \tag{13}$$

Substituting (5) into (12), we obtain the PDE, which is still dependent on the transversal coordinate x_3 ,

$$\left[k_H(\mathbf{x}) k_V(x_3) \left(\sum_{s=0}^{2} \left(\frac{x_3}{h}\right)^s \vartheta_s(\mathbf{x}, t)\right)_{,j}\right]_{,j} = 0 \ . \tag{14}$$

In order to get the pure 2D formulation, we can consider Eq. (14) in averaged sense over the plate thickness, which is physically meaningful as long as $L/h \gg 1$. Performing the integration of Eq. (14) over the plate thickness, we obtain the averaged heat conduction equation

$$\sum_{s=1}^{2} C^{(\theta\vartheta_s)}(\mathbf{x})\dot{\vartheta}_s^*(\mathbf{x},t) + \sum_{s=0}^{2} G_\beta^{(\theta\vartheta_s)}(\mathbf{x})\vartheta_{s,\beta}^*(\mathbf{x},t) + \sum_{s=0}^{2} G^{(\theta\vartheta_s)}(\mathbf{x})\vartheta_{s,\beta\beta}^*(\mathbf{x},t) = 0\,, \tag{15}$$

with

$$C^{(\theta\vartheta_a)}(\mathbf{x}) := \left(\frac{L}{h_0}\right)^2 \frac{k_H(\mathbf{x})}{\left(h^*(\mathbf{x})\right)^2}\left[k_V(1/2) + (-1)^a k_V(-1/2)\right] \tag{16}$$

$$G_\beta^{(\theta\vartheta_a)}(\mathbf{x}) := L\left(d_{(0)a} + \omega d_{(s)a}\right)k_{H,\beta}(\mathbf{x})\,, \quad G^{(\theta\vartheta_a)}(\mathbf{x}) := L^2\left(d_{(0)a} + \omega d_{(s)a}\right)k_H(\mathbf{x})\,.$$

Obviously, Eq. (15) is the PDE in 2D domain Ω and two additional equation result from the thermal boundary conditions on the bottom and top surfaces of the plate. Usually, we distinguish three kinds of thermal boundary conditions, which result into the following additional equations

(i) *Dirichlet type*: $\vartheta_0(\mathbf{x}) \pm \frac{1}{2}\vartheta_1(\mathbf{x}) + \frac{1}{4}\vartheta_2(\mathbf{x}) = \bar{\theta}(\mathbf{x}, \pm h/2) - \theta_0$ (17a)

(ii) *Neumann type*: $\mp k_0 k_H(\mathbf{x}) k_V(\pm h/2)\left[\vartheta_1(\mathbf{x}) \pm \vartheta_2(\mathbf{x})\right] = h\bar{q}(\mathbf{x}, \pm h/2)$ (17b)

(iii) *Robin type*: $A\left[1 + \vartheta_0(\mathbf{x}) \pm \frac{1}{2}\vartheta_1(\mathbf{x}) + \frac{1}{4}\vartheta_2(\mathbf{x})\right] \pm Bhk_0 k_H(\mathbf{x}) k_V(\pm h/2)\left[\vartheta_1(\mathbf{x}) \pm \vartheta_2(\mathbf{x})\right] = 0$ (17c)

in which $\bar{\theta}(\mathbf{x}, \pm h/2)$ and $\bar{q}(\mathbf{x}, \pm h/2)$ stand for the prescribed temperature and heat flux on the top and bottom surfaces of the plate.

Finally, the PDE (15) is to be supplemented with the boundary conditions on the boundary edge of the plate. Since $\theta(\mathbf{x}, x_3 = 0) = \theta_0 + \vartheta_0(\mathbf{x})$, the boundary conditions on $\partial\Omega$ can be given as

(i) *Dirichlet type*: $\vartheta_0(\mathbf{x})\big|_{\partial\Omega} = \bar{\theta}(\mathbf{x}, x_3 = 0) - \theta_0$ (18a)

(ii) *Neumann type*: $-k_0 k_H(\mathbf{x}) k_V(0) n_\beta(\mathbf{x}) \vartheta_{0,\beta}(\mathbf{x})\big|_{\partial\Omega} = \bar{q}(\mathbf{x}, 0)$ (18b)

(iii) *Robin type*: $A\vartheta_0(\mathbf{x})\big|_{\partial\Omega} + Bk_0 k_H(\mathbf{x}) k_V(0) n_\beta(\mathbf{x}) \vartheta_{0,\beta}(\mathbf{x})\big|_{\partial\Omega} = 0$. (18c)

in which $\bar{\theta}(\mathbf{x}, x_3 = 0)$ and $\bar{q}(\mathbf{x}, 0)$ are the prescribed values of the temperature and heat flux, respectively, on the boundary edge of the plate.

Note that the governing equations involve the 4th order derivatives of deflections and 3rd order derivatives of in-plane displacements and rotations. Since the accuracy of approximations of derivatives is decreasing with increasing the order of derivatives, we propose the decomposition of the derived system of the PDE into a set of PDE with derivatives not higher than the 2nd order by introducing new field variables [4] as

$$m(\mathbf{x}) := \nabla^2 w(\mathbf{x})\,, \quad s_\alpha(\mathbf{x}) := \nabla^2 u_\alpha(\mathbf{x})\,, \quad f_\alpha(\mathbf{x}) := \nabla^2 \varphi_\alpha(\mathbf{x})\,. \tag{19}$$

Summarizing, the governing equations for thermal problem are given by Eqs. (15) and (17) at $\mathbf{x} \in \Omega$ and the possible boundary conditions on $\partial\Omega$ are given by Eq. (18). The governing equations for the mechanical part of the thermo-elastic problem are given by Eqs. (8) and (19) at $\mathbf{x} \in \Omega$, while the possible boundary conditions can be properly constructed from Eq. (9).

Numerical implementation

Although the proposed decomposition of the original system of high-order PDE of elliptic type into the system of 2nd order PDE increases the number of field variables and finally the size of the matrix of discretized equations, it brings the possibility to solve the system of the decomposed PDE using the strong formulation which accelerates the computation significantly as compared with the weak formulation especially in case of utilization of meshless approximations, because the evaluations of shape functions is localized to nodal points. The functional in-plane gradation of material coefficients leads to the PDE with variable coefficients and the classical element-based discretization methods are mostly disqualified for efficient treatment of such rather complex problems. In order to simplified the mathematical complexity as much as possibly with preserving the physical nature of the solved problems, we propose to utilize the strong formulation and the meshless approximation of spatial variations of field variables, which is in this paper, the Moving Least Square approximation [5]. The nodal points are freely distributed in the analyzed domain and on its boundary without creating any connectivity among the nodes. Without going into details [6, 7], the approximation of a field variable $g(\mathbf{x})$ and its derivatives around the central approximation node $\mathbf{x}^q$ can be expressed by

$$g(\mathbf{x}) \approx \sum_{a=1}^{N^q} \hat{g}^{\bar{a}} \phi^{(q,a)}(\mathbf{x}) , \quad g_{,\alpha}(\mathbf{x}) \approx \sum_{a=1}^{N^q} \hat{g}^{\bar{a}} \phi^{(q,a)}_{,\alpha}(\mathbf{x}) , \quad g_{,\alpha\beta}(\mathbf{x}) \approx \sum_{a=1}^{N^q} \hat{g}^{\bar{a}} \phi^{(q,a)}_{,\alpha\beta}(\mathbf{x}) , \tag{20}$$

where $\bar{a} = n(q,a)$ is the global number of the a-th node from the influence domain of $\mathbf{x}^q$, N^q is the number of nodal points in the influence domain, which is smaller than the total number of nodes, and $\phi^{(q,a)}(\mathbf{x})$ is the shape function associated with the node $n(q,a)$. This shape function is not known in a closed form [8], but it must be evaluated at each point $\mathbf{x}$. Recall that $\hat{g}^{\bar{a}}$ is the nodal unknown associated with the node $\bar{a}$ and is different from the nodal value $g(\mathbf{x}^{\bar{a}})$. The central approximation node can be selected as the nearest node to the field point $\mathbf{x}$. For creation of shape functions, we have used cubic monomial basis and Gaussian weights.

In the strong formulation, the governing equations are collocated at interior nodes and the boundary conditions at boundary nodes.

Numerical examples

In numerical investigations, we consider a square plate $L \times L$ with $L = 1$ and the results are presented for dimensionless quantities specified as:

$$x_\beta^* := \frac{x_\beta}{L} , \quad x_3^* := \frac{x_3}{h_0} = h^*(\mathbf{x}) z , \quad u_\beta^*(\mathbf{x}^*) := \frac{u_\beta(\mathbf{x})}{h_0} , \quad \varphi_\beta^*(\mathbf{x}^*) := \varphi_\beta(\mathbf{x}) , \quad w^*(\mathbf{x}^*) := \frac{w(\mathbf{x})}{h_0} ,$$

$$\vartheta_s^*(\mathbf{x}^*) := \frac{\vartheta_s(\mathbf{x})}{\theta_0} , \quad t_3^*(\mathbf{x}^*) := \frac{L^4}{D_0 h_0} t_3(\mathbf{x}) \ , \ \text{with}\ D_0 = \frac{E_0 (h_0)^3}{12(1-\nu^2)} .$$

In what follows, we shall omit the superscript * in dimensionless Cartesian coordinates.
In all numerical computations, we have used a uniform distribution of nodal points (36 x36 nodes) with δ being the distance between two neighbour nodes. The other parameters in the MLS-approximation with Gaussian weights have been taken as: the radius of the influence domain $\rho^a = 3.001\delta$, shape function parameter $c^a = \delta$, and cubic monomial basis. Note that

the number of nodes falling into the influence domain of a global node varies from 11 to 27 depending on the position of the global node.

Elasto-static simulations

We start the study of coupling effects due to continuously variable: (i) Young's modulus in transversal direction $E_V(x_3)=1+\zeta\left(1/2\pm x_3/h\right)^p$; (ii) in-plane gradations of Young's modulus $E_H(\mathbf{x})=1+\kappa_0\left(x_1/L\right)^{b_0}$; (iii) variable plate thickness $h^*(\mathbf{x})=1+\kappa\left(x_1/L\right)^s$. The Poisson ratio is assumed to be constant $\nu=0.3$. The boundary edges of the plate are clamped and the plate is subjected to uniform transversal loading $t_3^*(\mathbf{x})=1$.
The influence of thickness of the plate on deflections is shown in Fig.1 for homogeneous plate. It is seen that the KLT is applicable only to thin plates $L/h_0>50$, when the deviation of the KLT results from those by the SDPT is less than 1%.

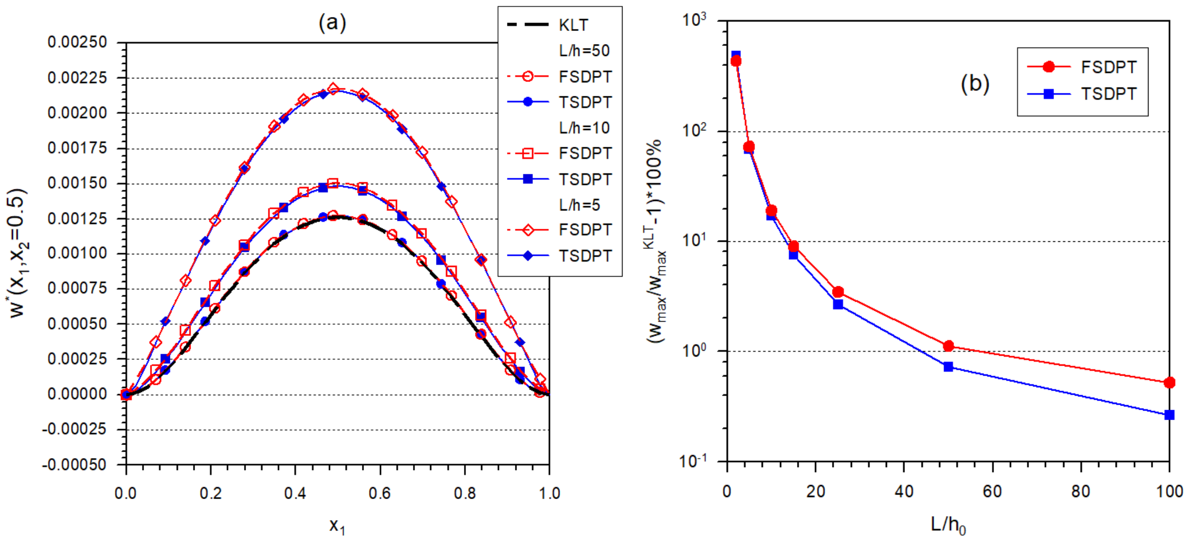

Figure 1. Comparison of deflections by KLT and SDPT: (a) deflections along x_1-axis; (b) % deviations vs. ratio of length to thickness

Fig. 2 shows the response of three thin plates (homogeneous and FGM plates with 2 different levels of gradation of Young's modulus, $\zeta=1$ and $\zeta=3$) to uniform transversal loading. The evidence of coupling between the bending and in-plane deformation modes is clearly seen from Fig. 2(c), since finite in-plane displacements arise only in FGM plates.

The influence of the in-plane power-law gradation of Young's modulus on the response of thick plate is shown in Fig. 3. It is seen that deflections are affected more expressively by the level of gradation than by the exponent of gradation. This can be explained by the effect of lower bulk content of the material with higher value of the Young modulus. The shift of maximal deflections toward the softer side of the plate is evident.

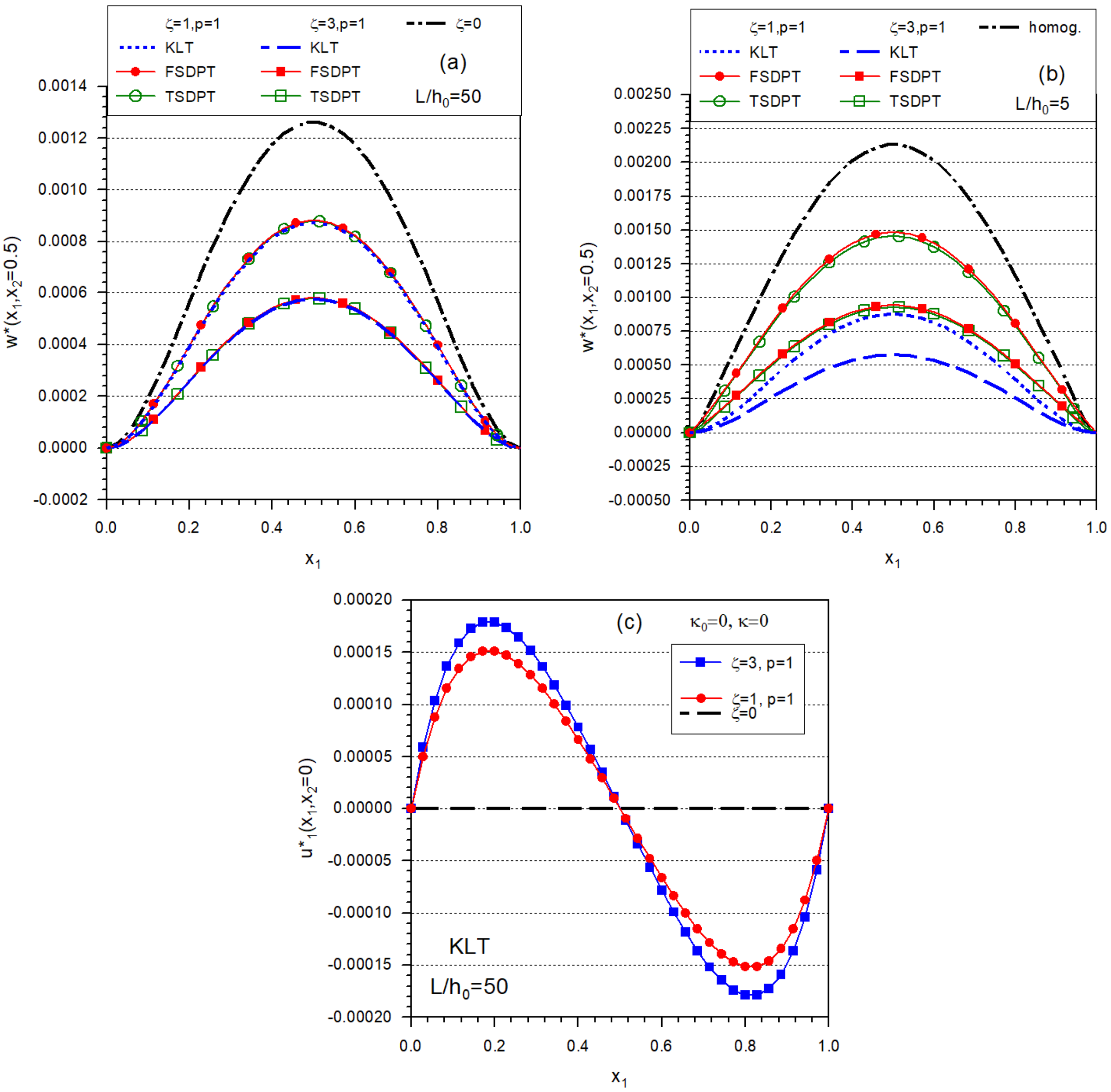

Figure 2. The response of three plates by various theories. In-plane distribution: (a) deflections of thin plate; (b) deflections of thick plate; (c) in-plane displacements

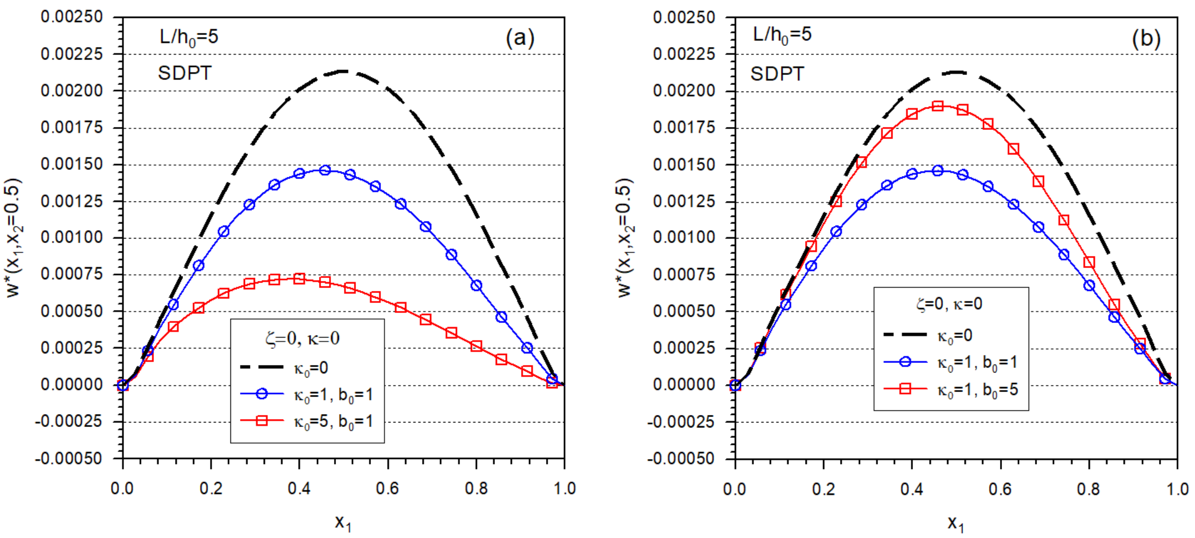

Figure 3. Influence of in-plane gradation of Young's modulus on the response of thick FGM plate. The effects by: (a) different levels of gradation; (b) different exponents of power-law gradation

Form Fig. 4(a), it can be seen that the influence of levels of linear in-plane gradations of plate thickness on deflections is more significant than the influence of gradation of Young's modulus. The negative effect of thinning the plate can be compensated or suppressed by parallel gradual increasing the Young modulus with resulting in overall reduction of deflection (Fig. 4(b)).

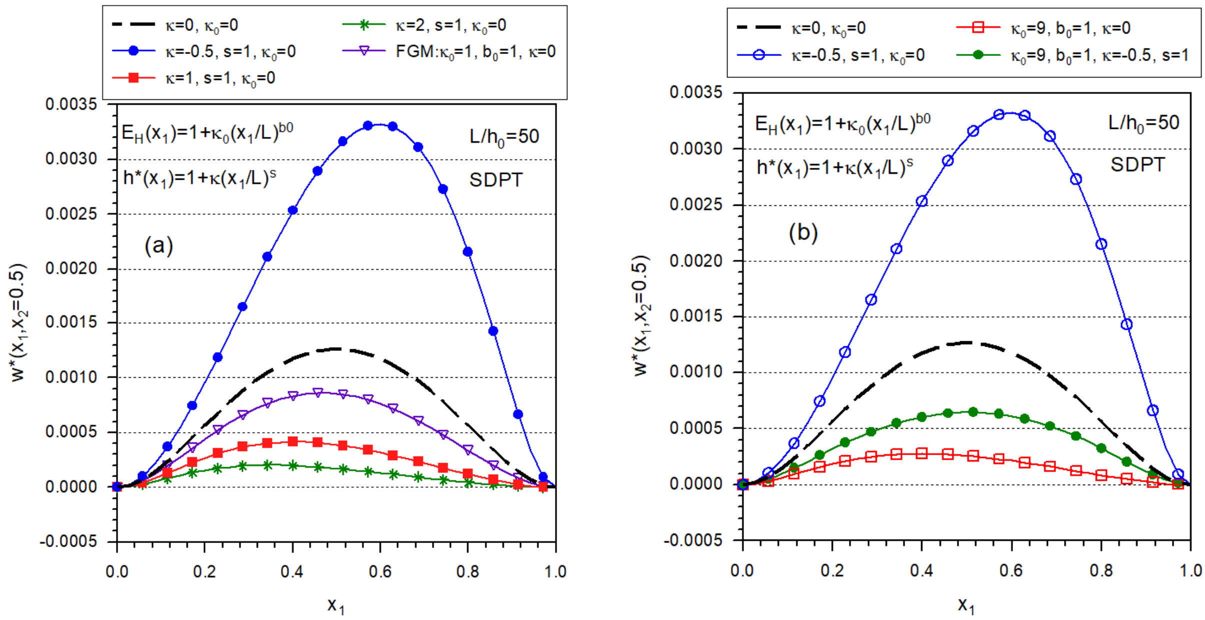

Figure 4. Response of plates with variable parameters of in-plane gradations: (a) κ and/or κ_0; (b) κ and/or κ_0 including combined gradations of Young's modulus and plate thickness

Now, we shall continue in numerical simulations and study of multi-gradation effects in square FGM elastic plates with transversal gradation of Young's modulus $E_V(x_3) = 1 + \zeta\left(1/2 \pm x_3/h\right)^p$ combined with: (i) in-plane gradation of Young's modulus $E_H(\mathbf{x}) = 1 + \kappa_0\left(x_1/L\right)^{b_0}$; (ii) in-plane continuous variation of plate thickness $h^*(\mathbf{x}) = 1 + \kappa\left(x_1/L\right)^s$; (iii) simultaneous in-plane gradations of Young's modulus and plate thickness. The plate is subject to uniform in-plane tension $T^*_{\alpha 1}(x_1 = 1, x_2) = \delta_{\alpha 1} h_0 h^*(x_1 = 1, x_2)$, and the boundary conditions on the other edges are given as: $u^*_1(x_1 = 0, x_2) = 0$, $T^*_{21}(x_1 = 0, x_2) = 0$, $T^*_{\alpha 2}(x_1, x_2 = 0) = T^*_{\alpha 2}(x_1, x_2 = 1) = 0$, with assuming two alternatives for bending modes:

- clamped boundary edges

$$w^*(\mathbf{x})\Big|_{\partial\Omega} = 0\,,\quad \frac{\partial w^*(\mathbf{x})}{\partial \mathbf{n}}\bigg|_{\partial\Omega} = 0\,,\quad \varphi^*_\alpha(\mathbf{x})\Big|_{\partial\Omega} = 0\,,\quad t^*_3(\mathbf{x}) = 0$$

- simply supported edges

$$w^*(\mathbf{x})\Big|_{\partial\Omega} = 0\,,\; n_\alpha(\mathbf{x}) n_\beta(\mathbf{x}) M^{(w)*}_{\alpha\beta}(\mathbf{x})\Big|_{\partial\Omega} = 0\,,\; n_\beta(\mathbf{x}) M^{(\varphi)*}_{\alpha\beta}(\mathbf{x})\Big|_{\partial\Omega} = 0\,,\; t^*_3(\mathbf{x}) = 0\,.$$

The in-plane loading doesn't yield finite deflections in homogeneous as well as FGM with only transversal gradation of Young's modulus.

Firstly consider the FGM plates with clamped sliding edges. Fig. 5 show the in-plane displacements and deflections in thin FGM plates with combined gradations of Young's modulus for various levels and/or exponents of in-plane gradation. The combined gradation of Young's modulus is sufficient for arising finite deflections in FGM plates subject to in-plane tension.

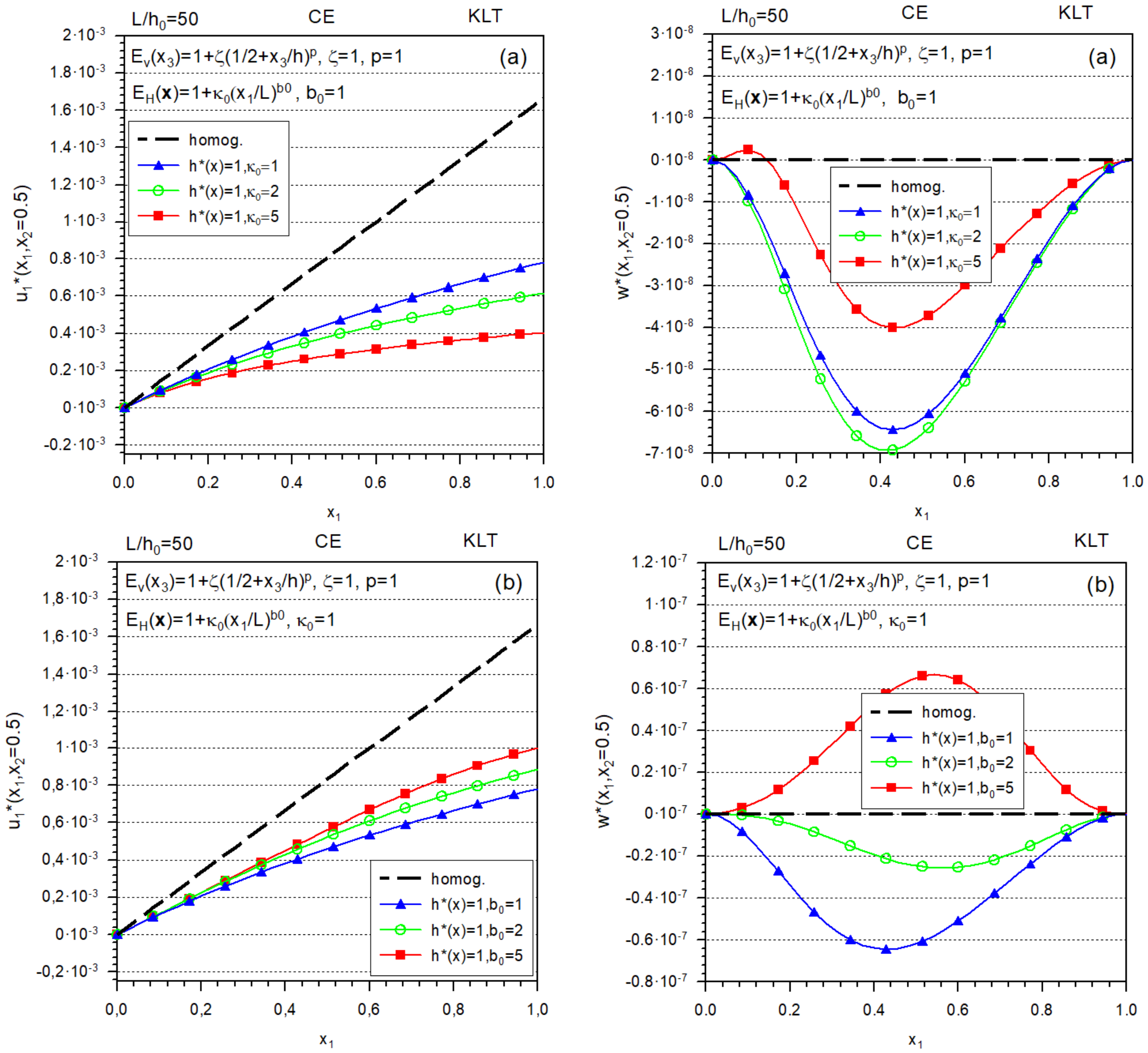

Figure 5. Influence of gradation parameters: (a) levels of gradations; (b) exponents of gradations on in-plane displacements and deflections in thin FGM plates with combined transversal and in-plane gradations of Young's modulus

Numerical simulations indicate that similar behavior is observed also in FGM plates with transversal gradation of Young's modulus and continuously variable thickness (Fig. 6). Note that the nonlinear gradation of the plate thickness leads to more significant deflection response than in the case of linear gradation.

Note that in the case of thin plates, the KLT results are almost identical with those by SDPT. However, in the case of thick plates, it is necessary to use the TSDPT. More remarkable deflection response to in-plane loading is observed in the case of thick plates if $s=1$ (Fig. 7).

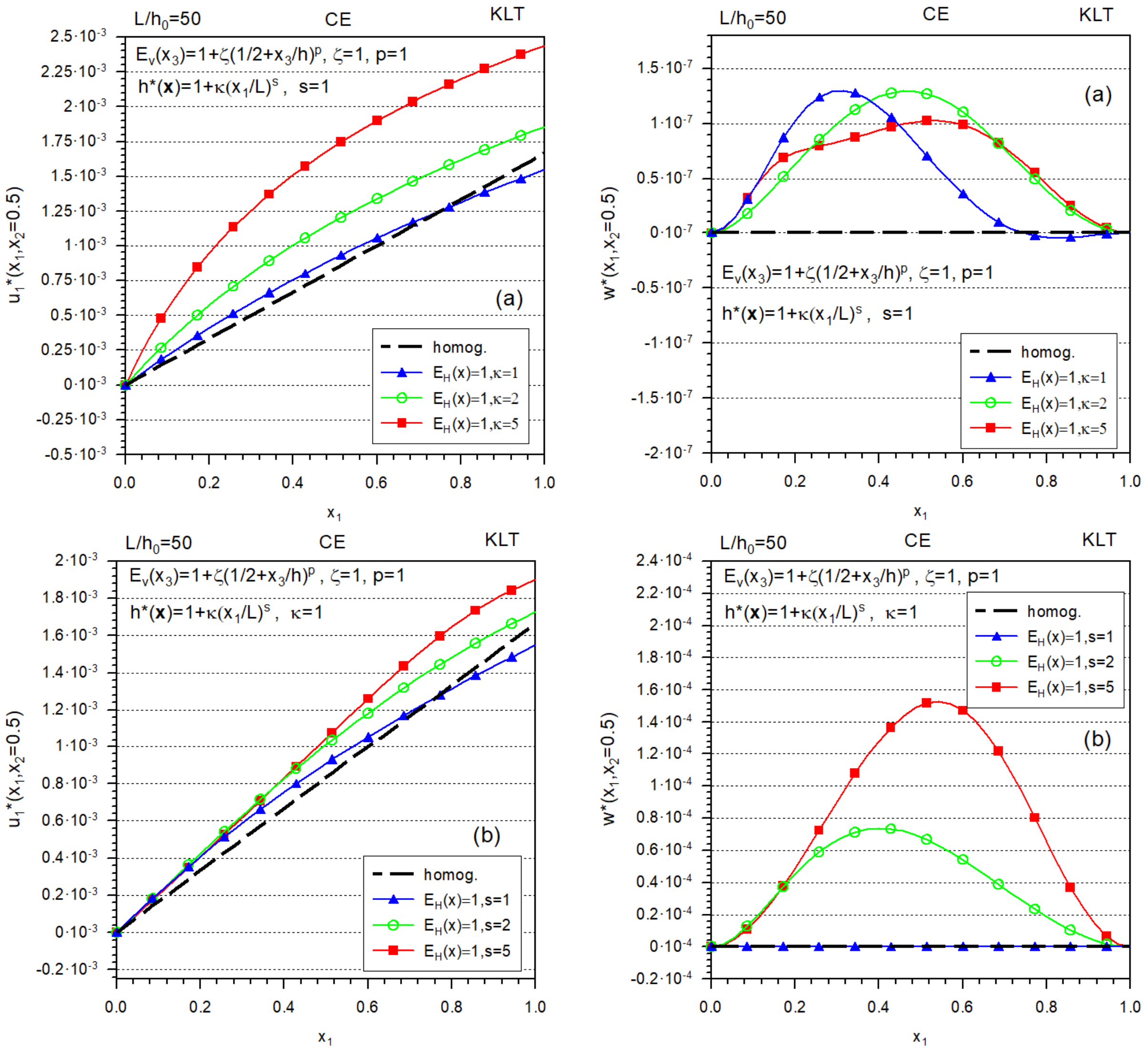

Figure 6. Influence of gradation parameters: (a) levels of gradations; (b) exponents of gradations on in-plane displacements and deflections in thin FGM plates with combined transversal gradation of Young's modulus and in-plane variation of plate thickness

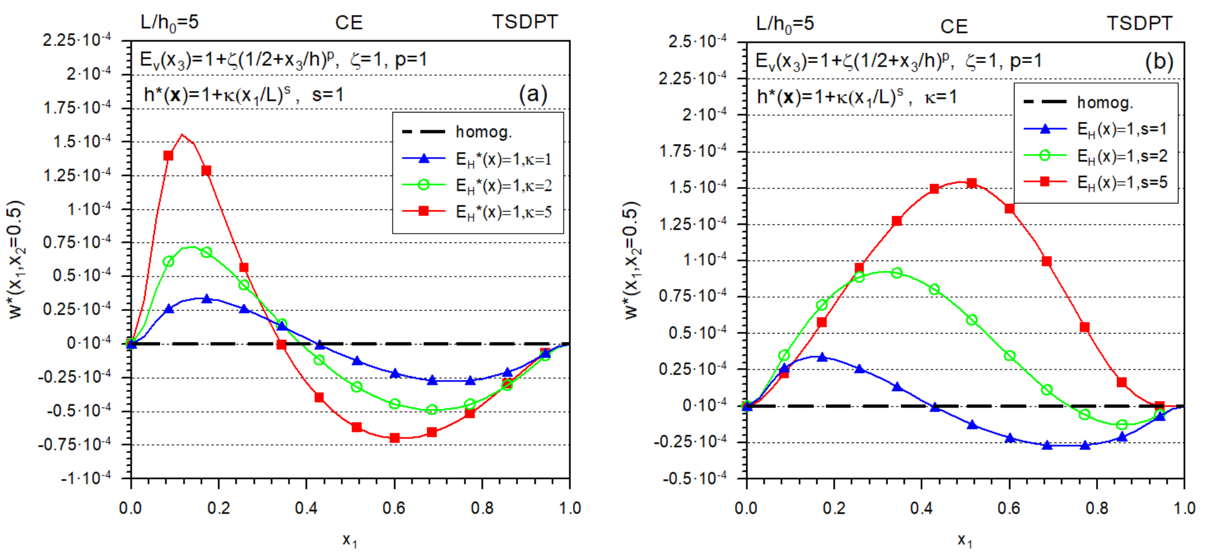

Figure 7. Influence of gradation parameters: (a) levels of gradations; (b) exponents of gradations on deflections of thick FGM plates with combined transversal gradation of Young's modulus and in-plane variation of plate thickness

In the rest of the elastostatical subsection, we shall consider FGM plates with simply supported sliding edges. Now, the transversal gradation of Young's modulus is sufficient for finite deflection response, in contrast to the plates with clamped sliding edges (Fig.8). For more details, we refer the reader to the work [9].

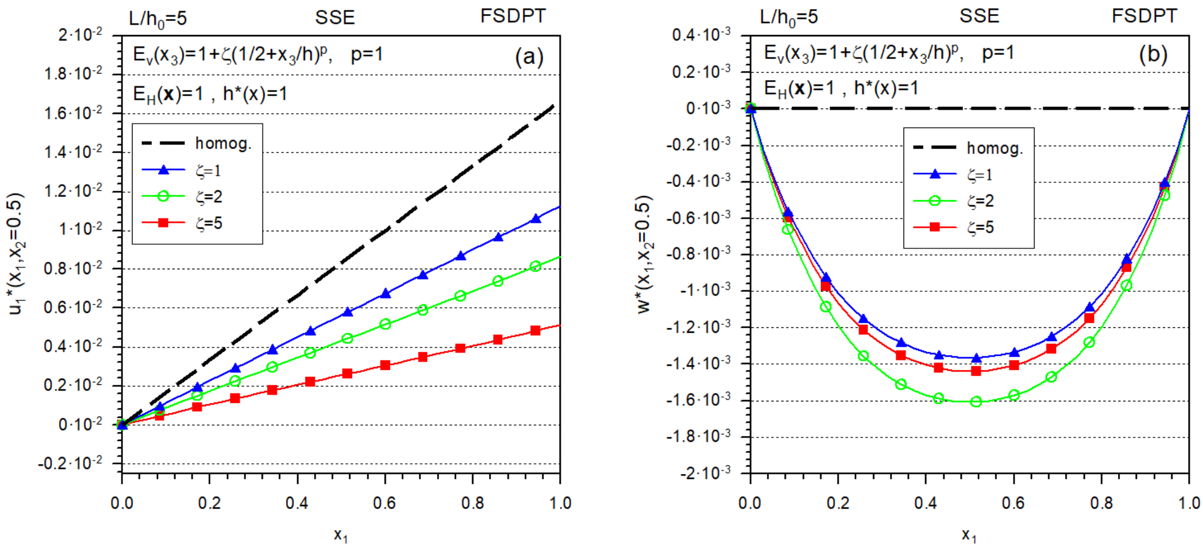

Figure 8. Influence of the level of linear transversal gradation of Young's modulus on the response of the FGM plates with SSE to in-plane tension: (a) in-plane displacements; (b) deflections

The numerical simulations in the FGM plates with combined gradations and simply supported edges (SSE) resembles qualitatively those in the FGM plates with multi-gradation and clamped edges (CE). However, the deflection response in FGM plates with SSE is much more expressive than that in the FGM plates with multi-gradation and CE. Finally, the results for the FGM plates with variable thickness and combined transversal and in-plane gradations of Young's modulus are illustrated in Fig.9.

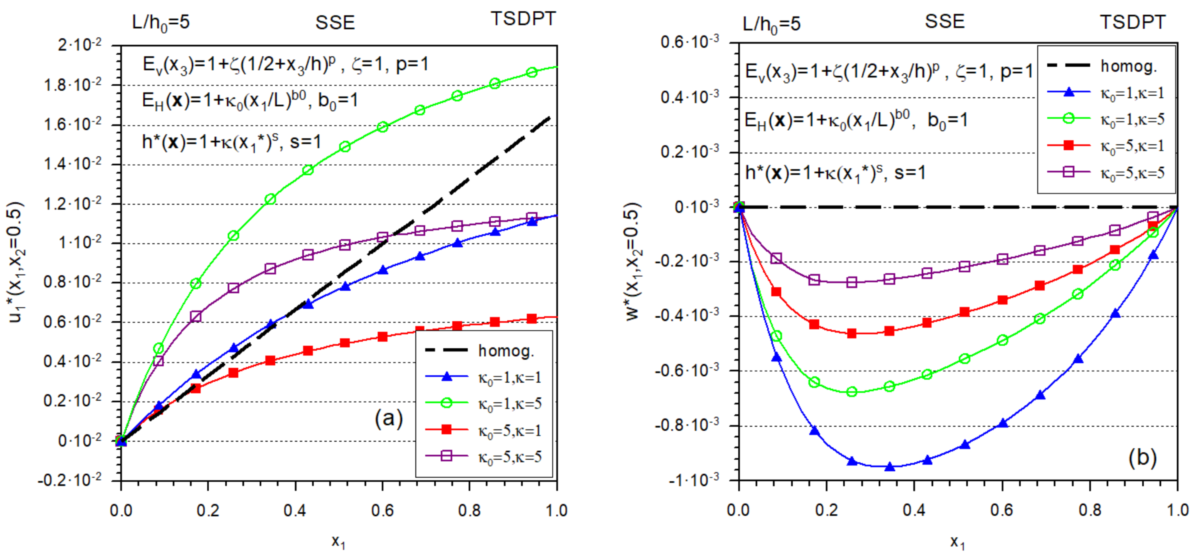

Figure 9. Influence of the multi-gradations of Young's modulus and plate thickness on the response of the FGM plates with SSE to in-plane tension: (a) in-plane displacements; (b) deflections

Thermo-elastic simulations

In addition to functional gradation of elasticity coefficients, we assume the transversal gradation of the linear thermal expansion and the heat conduction coefficients specified by Eqs. (4) and (13), and the following in-plane power-law gradations

$$\alpha_H(\mathbf{x}) = 1 + \kappa_1 (x_1 / L)^{b_1}, \quad k_H(\mathbf{x}) = 1 + \kappa_2 (x_1 / L)^{b_2}.$$

The natural thermal boundary conditions are assumed on the bottom and top surfaces of plate

$$\theta(\mathbf{x}, \pm h/2) = \theta^{\pm} \text{ with } \theta_0 = 1, \; \theta^+ = \theta_0 + 20, \quad \theta^- = \theta_0$$

and heat flux is assumed to be vanishing on the boundary edges of the plate

$$-k_0 k_H(\mathbf{x}) k_V(0) n_\beta(\mathbf{x}) \vartheta_{0,\beta}(\mathbf{x})\Big|_{\partial\Omega} = \bar{q}(\mathbf{x}, 0) = 0.$$

Then, the temperature field is distributed uniformly within the mid-plane Ω and the value of the temperature is affected only by the level of gradation of the heat conduction coefficient, ω . The numerical simulations presented in Fig. 10 show that the KLT and TSDPT give different response of the FGM plates with clamped edges (CE) to considered thermal loading even if the plates are thin. It can be seen from the analysis of the governing equations [10] that there is a coupling between deflections and thermal fields in the KLT only if $\nabla^2 \left(E_H(\mathbf{x}) \alpha_H(\mathbf{x}) \right) \neq 0$ while in the case of the SDPT such a coupling appears even if $\nabla \left(E_H(\mathbf{x}) \alpha_H(\mathbf{x}) \right) \neq 0$.

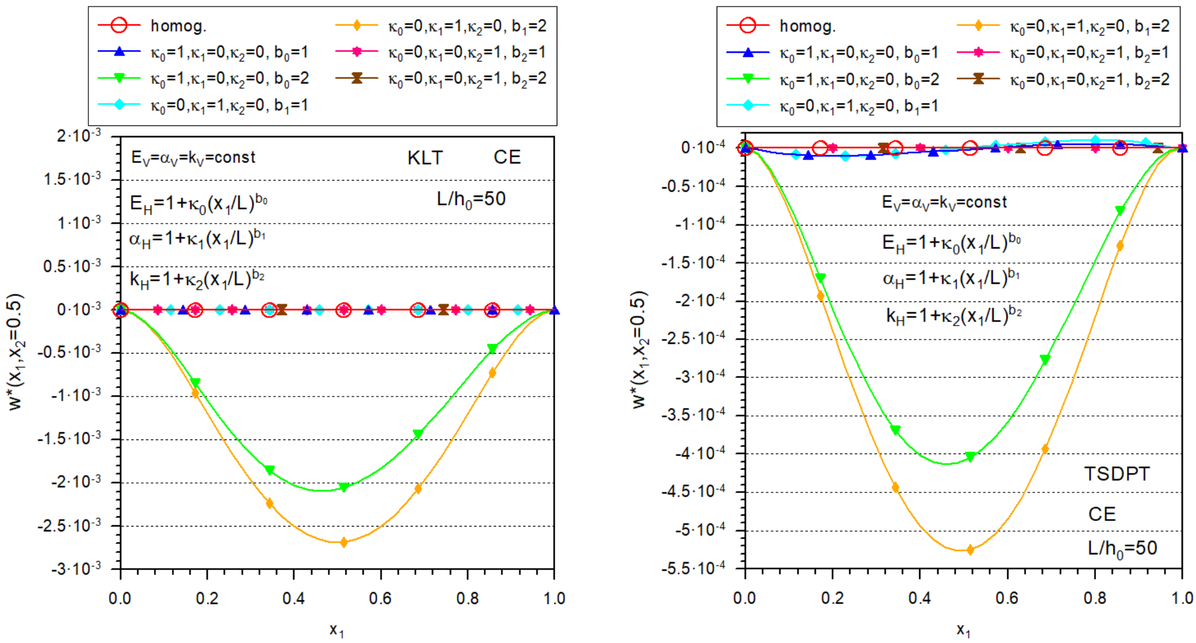

Figure 10. Deflection response to thermal loading in FGM plates with in-plane gradation of material coefficients and clamped edges

The plates with simply supported edges (SSE) exhibit quite different behavior as plates with clamped edges. One observes finite deflections also in homogeneous plates with SSE, because the thermal contribution to the bending moment, $n_\alpha n_\beta M^{*(w\theta)}_{\alpha\beta} = n_\alpha n_\beta \sum_{a=0}^{2} C^{(w\vartheta_a)} \tau^{*(\vartheta_a)}_{\alpha\beta}$, on the boundary edge is compensated by contribution associated with deflection strains, i.e. $n_\alpha n_\beta M^{*(w\theta)}_{\alpha\beta}$ is the boundary source for $n_\alpha n_\beta M^{*(ww)}_{\alpha\beta} = n_\alpha n_\beta \sum_{a=0}^{2} C^{(ww)} \tau^{*(w)}_{\alpha\beta}$. On the other hand, such thermal source is ineffective on the clamped edge.

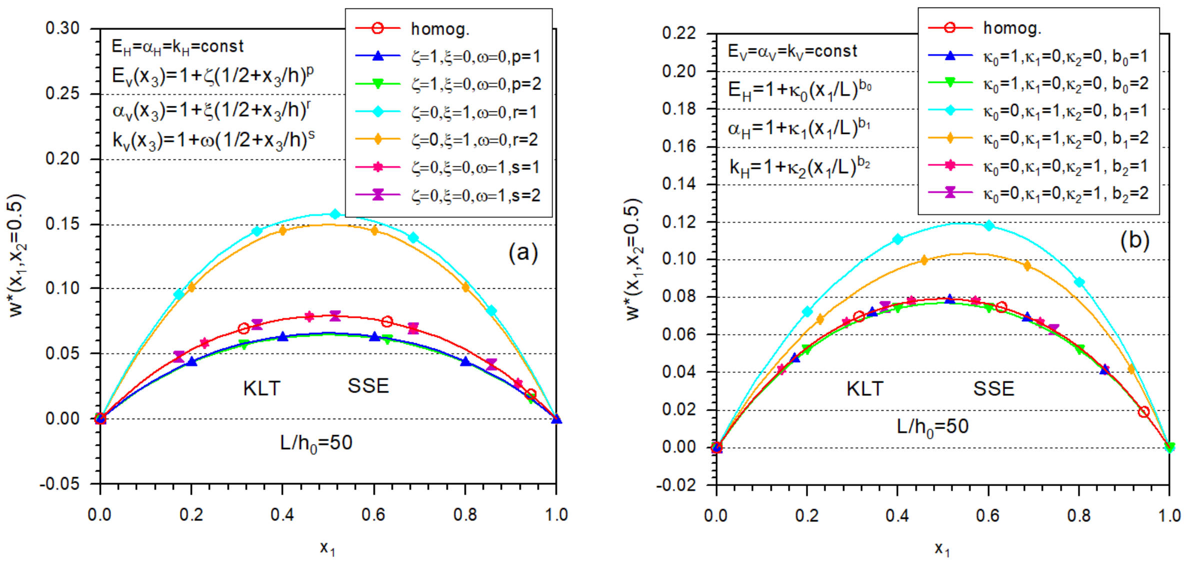

Figure 11. Deflection response to thermal loading in FGM plates with simply supported edges and various gradations of material coefficients: (a) transversal gradation; (b) in-plane gradation

The influence of gradation of material coefficients on the deflection responses in FGM plates with simply supported edges are shown in Fig. 11. It is seen that deflection response is much more expressive than in the case of plates with clamped edges.

Conclusions

The unified formulation for FGM plates is developed within stationary thermo-elasticity with including the assumptions of the Kirchhoff-Love theory as well as the 1st and 3rd order shear deformation plate theories. The functional gradation is considered in the transversal and/or in-plane direction for such material coefficients as: the Young modulus, coefficient of linear thermal expansion, and heat conduction coefficient. Moreover, the plate thickness can be continuously variable too. For the derived 2D formulation, the numerical implementation is developed with making use the strong formulation and meshless approximation of spatial variations of field variables. The original system of the governing PDE is decomposed into the system of the 2nd order PDE, in order to decrease the order of derivatives in the original system. The numerical simulations are employed for study the coupling effects in FGM plates subjected to three kinds of stationary loading: (i) uniform transversal mechanical loading; (ii) simple tension applied in the plane of plate; (iii) thermal loading. Individual as well as combined gradations of material coefficients and the plate thickness are considered. The coupling between the bending and in-plane deformation modes is explained and particular coupling effects are documented and discussed.

Acknowledgements

The financial support of the Slovak Research and Development Agency under the contract No. APVV-14-0440 is greatly acknowledged.

Appendix

The integrations required in definition of semi-integral fields can be performed in closed form and expressed in terms of two kinds of integrals

$$d_{(0)a} := \int_{-1/2}^{1/2} z^a dz = \frac{1+(-1)^a}{(a+1)2^{a+1}} \tag{A.1}$$

$$d_{(p)a} := \int_{-1/2}^{1/2} z^a \left(\frac{1}{2} \pm z\right)^p dz = (\pm 1)^a \int_0^1 \left(y - \frac{1}{2}\right)^a y^p dy = (\pm 1)^a \sum_{k=0}^{a} \binom{a}{k} \left(-\frac{1}{2}\right)^k \frac{1}{p+1+a-k}$$

In view of the definitions (10), (3), (6) and (A.1), the semi-integral fields are given as

$$T_{\alpha\beta}(\mathbf{x}) = C^{(uu)}(\mathbf{x})\tau_{\alpha\beta}^{(u)}(\mathbf{x}) + C^{(u\varphi)}(\mathbf{x})\tau_{\alpha\beta}^{(\varphi)}(\mathbf{x}) + C^{(uw)}(\mathbf{x})\tau_{\alpha\beta}^{(w)}(\mathbf{x}) + \sum_{a=0}^{2} C^{(u\vartheta_a)}(\mathbf{x})\tau_{\alpha\beta}^{(\vartheta_a)}(\mathbf{x}) \tag{A.2}$$

$$T_{3\alpha}^{(w\varphi)}(\mathbf{x}) = C^{s}(\mathbf{x})\left[w_{,\alpha}(\mathbf{x}) + \varphi_{\alpha}(\mathbf{x})\right]$$

$$M_{\alpha\beta}^{(\varphi)}(\mathbf{x}) = C^{(\varphi u)}(\mathbf{x})\tau_{\alpha\beta}^{(u)}(\mathbf{x}) + C^{(\varphi\varphi)}(\mathbf{x})\tau_{\alpha\beta}^{(\varphi)}(\mathbf{x}) + C^{(\varphi w)}(\mathbf{x})\tau_{\alpha\beta}^{(w)}(\mathbf{x}) + \sum_{a=0}^{2} C^{(\varphi\vartheta_a)}(\mathbf{x})\tau_{\alpha\beta}^{(\vartheta_a)}(\mathbf{x})$$

$$M_{\alpha\beta}^{(w)}(\mathbf{x}) = C^{(wu)}(\mathbf{x})\tau_{\alpha\beta}^{(u)}(\mathbf{x}) + C^{(w\varphi)}(\mathbf{x})\tau_{\alpha\beta}^{(\varphi)}(\mathbf{x}) + C^{(ww)}(\mathbf{x})\tau_{\alpha\beta}^{(w)}(\mathbf{x}) + \sum_{a=0}^{2} C^{(w\vartheta_a)}(\mathbf{x})\tau_{\alpha\beta}^{(\vartheta_a)}(\mathbf{x})$$

with the coefficients $C^{(\bullet\bullet)}(\mathbf{x})$ being given as

$$C^{(uu)}(\mathbf{x}) := 12\frac{1-\nu}{H}\frac{D_0}{(h_0)^2}\left(d_{(0)0} + \zeta d_{(p)0}\right)D_{1H}(\mathbf{x}) \tag{A.3}$$

$$C^{(u\varphi)}(\mathbf{x}) := 12\frac{1-\nu}{H}\frac{D_0}{h_0}c_1\zeta\left(d_{(p)1} - \frac{4}{3}c_2 d_{(p)3}\right)D_{2H}(\mathbf{x}) = C^{(\varphi u)}(\mathbf{x})$$

$$C^{(uw)}(\mathbf{x}) := 12\frac{1-\nu}{H}\frac{D_0}{h_0}\zeta\left[(c_1-1)d_{(p)1} - \frac{4}{3}c_1 c_2 d_{(p)3}\right]D_{2H}(\mathbf{x})$$

$$C^{(u\vartheta_a)}(\mathbf{x}) := -12\frac{1-\nu}{H}\frac{D_0}{(h_0)^2\theta_0}\alpha_0\theta_0\left(d_{(0)a} + \xi d_{(r)a} + \zeta d_{(p)a} + \xi\zeta d_{(p+r)a}\right)B_{1H}(\mathbf{x})$$

$$C^{s}(\mathbf{x}) := c_1 6(1-\nu)\frac{D_0}{(h_0)^2}\Big\{\left[(1-c_2)\kappa + c_2\right]\left(d_{(0)0} + \zeta d_{(p)0}\right) - 8c_2\left(d_{(0)2} + \zeta d_{(p)2}\right) + \\ +16c_2\left(d_{(0)4} + \zeta d_{(p)4}\right)\Big\}D_{1H}(\mathbf{x})$$

$$C^{(\varphi\varphi)}(\mathbf{x}) := 12\frac{1-\nu}{H}D_0 c_1\Big[d_{(0)2} - \frac{8}{3}c_2 d_{(0)4} + \frac{16}{9}c_2 d_{(0)6} + \\ +\zeta\left(d_{(p)2} - \frac{8}{3}c_2 d_{(p)4} + \frac{16}{9}c_2 d_{(p)6}\right)\Big]D_{3H}(\mathbf{x})$$

$$C^{(\varphi w)}(\mathbf{x}) := -16\frac{1-\nu}{H}D_0 c_1 c_2\left[d_{(0)4} - \frac{4}{3}d_{(0)6} + \zeta\left(d_{(p)4} - \frac{4}{3}d_{(p)6}\right)\right]D_{3H}(\mathbf{x})$$

$$C^{(\varphi\vartheta_a)}(\mathbf{x}) := -12\frac{1-\nu}{H}\frac{D_0}{h_0\theta_0}\alpha_0\theta_0 c_1\left[d_{(0)a+1} - \frac{4}{3}c_2 d_{(0)a+3} + \xi\left(d_{(r)a+1} - \frac{4}{3}c_2 d_{(r)a+3}\right) + \right.$$

$$\left. + \zeta\left(d_{(p)a+1} - \frac{4}{3}c_2 d_{(p)a+3}\right) + \xi\zeta\left(d_{(p+r)a+1} - \frac{4}{3}c_2 d_{(p+r)a+3}\right)\right]B_{2H}(\mathbf{x})$$

$$C^{(wu)}(\mathbf{x}) := 12\frac{1-\nu}{H}\frac{D_0}{h_0}\zeta\left[(1-c_1)d_{(p)1} + \frac{4}{3}c_1 c_2 d_{(p)3}\right]D_{2H}(\mathbf{x}) = -C^{(uw)}(\mathbf{x})$$

$$C^{(w\varphi)}(\mathbf{x}) := 16\frac{1-\nu}{H}D_0 c_1 c_2\left[d_{(0)4} - \frac{4}{3}d_{(0)6} + \zeta\left(d_{(p)4} - \frac{4}{3}d_{(p)6}\right)\right]D_{3H}(\mathbf{x}) = -C^{(\varphi w)}(\mathbf{x})$$

$$C^{(ww)}(\mathbf{x}) := 12\frac{1-\nu}{H}D_0\left\{(c_1-1)d_{(0)2} - \frac{16}{9}c_1 c_2 d_{(0)6} + \zeta\left[(c_1-1)d_{(p)2} - \frac{16}{9}c_1 c_2 d_{(p)6}\right]\right\}D_{3H}(\mathbf{x})$$

$$C^{(w\vartheta_a)}(\mathbf{x}) := 12\frac{1-\nu}{H}\frac{D_0}{h_0\theta_0}\alpha_0\theta_0\left\{(c_1-1)d_{(0)a+1} - \frac{4}{3}c_1 c_2 d_{(0)a+3} + \right.$$

$$+\xi\left[(c_1-1)d_{(r)a+1} - \frac{4}{3}c_1 c_2 d_{(r)a+3}\right] + \zeta\left[(c_1-1)d_{(p)a+1} - \frac{4}{3}c_1 c_2 d_{(p)a+3}\right] +$$

$$\left. +\xi\zeta\left[(c_1-1)d_{(p+r)a+1} - \frac{4}{3}c_1 c_2 d_{(p+r)a+3}\right]\right\}B_{2H}(\mathbf{x})$$

where $D_{jH}(\mathbf{x}) := \left(h^*(\mathbf{x})\right)^j E_H(\mathbf{x})$, $B_{jH}(\mathbf{x}) := \left(h^*(\mathbf{x})\right)^j E_H(\mathbf{x})\alpha_H(\mathbf{x})$, $h^*(\mathbf{x}) = h(\mathbf{x})/h_0$.

References

[1] Nowacki, W. (1975) *Dynamic Problems of Thermoelasticity*, Noordhoff International Publishing, Leyden, The Netherlands.

[2] Sator, L., Sladek, V., Sladek, J. (2014) Coupling effects in elastic analysis of FGM composite plates by mesh-free methods, *Composite Structures* **115**, 309–322.

[3] Sator, L., Sladek, V., Sladek, J. (2016) Elastodynamics of FGM plates by meshfree method, *Composite Structures* **140**, 100–110.

[4] Sladek, V., Sladek, J., Sator, L. (2013) Physical decomposition of thin plate bending problems and their solution by mesh-free methods, *Engineering Analysis with Boundary Elements* **37**, 348–365.

[5] Lancaster, P., Salkauskas, K. (1981) Surfaces generated by moving least square methods, *Math Comput* **37**, 141-158.

[6] Sladek, V., Sladek, J., Zhang, Ch. (2008) Computation of stresses in non-homogeneous elastic solids by local integral equation method: a comparative study, *Computational Mechanics* **41**, 827-845.

[7] Sladek, V., Sladek, J. (2010) Local integral equations implemented by MLS approximation and analytical integrations, *Engineering Analysis with Boundary Elements* **34**, 904-913.

[8] Atluri, S.N. (2004) *The meshless method, (MLPG) for domain & BIE discretization*, Tech. Science Press, Forsyth.

[9] Sator, L., Sladek, V., Sladek, J. (2017) Multi-gradation coupling effects in FGM plates, *Composite Structures* **171**, 515–527.

[10] Sladek, V., Sator, L., Sladek, J. (2018) Thermoelastic analysis of bending problems in FGM plates, *Int J Comp Meth and Exp Meas* **6**, 1161-1172.

[11] Bever, M.B., Duwez, P.E. (1972) Gradients in composite materials, *Mater Sci Eng* **10**, 1-8.

[12] Jha, D.K., Kant, T., Singh, R.K. (2013) A critical review of recent research on functionally graded plates, *Composite Structures* **96**, 833-849.

[13] Suresh, S., Mortensen, A. (1998) *Fundamentals of Functionally Graded Materials*, Institute of Materials, London.

[14] Koizumi, M. (1993) The concept of FGM, *Ceramic Transactions* **34**, 3-10.
[15] Yamanouchi, M., Koizumi, M. Hirai, T., Shioda, I. (1990) *Proceedings of the First International Symposium on Functionally Graded Materials*, FGM Forum, Tokyo.
[16] Reddy, J.N. *Mechanics of Laminated Composite Plates: Theory and Analysis*, CRC Press, Boca Raton.
[17] Tornabene, F. (2009) Free vibration analysis of functionally graded conical, cylindrical shell and annular plate structures with four-parameter power-law distribution, *Comput Meth Appl Mech Engng* **198**, 2911-2935.
[18] Tornabene, F., Viola, E. (2009) Free vibration of four-parameter functionally graded parabolic panels and shells of revolution, *Eur Jour Mech A/Solids* **28**, 991-1013.
[19] Tornabene, F., Fantuzzi, N., Bacciocchi, M., Viola, E, Reddy, J.N. (2017) A numerical investigation on the natural frequencies of FGM sandwich shells with variable thickness by the local generalized differential quadrature method, *Applied Sciences* **7**, 131.
[20] Ardestani, M.M., Soltani, B., Shams, S. (2014) Analysis of functionally graded stiffened plates based on FSDT utilizing reproducing kernel particle method, *Composite Structures* **112**, 231-240.
[21] Barber, J.R. (2010) *Elasticity*, Springer Science+Business Media B.V., New York.
[22] Lurie, A.I. (2005) *Theory of Elasticity*, Springer-Verlag, Berlin.
[23] Mantari, J.L., Oktem, A.S., Guedes Soares, C. (2012) Bending response of functionally graded plates by using a new higher order shear deformation theory, *Composite Structures* **94**, 714-723.